SINGLE LAYER GRAPHENE AS A STABLE AND TRANSPARENT ELECTRODE FOR THE MEASUREMENT OF NON-AQUEOUS ELECTROGENERATED CHEMILUMINESCENCE AND CHARGE TRANSFER INVERSE PHOTOEMISSION

BY

TERESA CECELIA CRISTARELLA

THESIS

Submitted in partial fulfillment of the requirements
for the degree of Master of Science in Chemistry
in the Graduate College of the
University of Illinois at Urbana-Champaign, 2014

Urbana, Illinois

Adviser:

Professor Joaquín Rodríguez-López

Abstract

In this work we explore the use of single layer graphene (SLG) obtained by chemical vapor deposition as a transparent electrode material for use in coupled electrochemical and spectroscopic experiments in non-aqueous media through electrogenerated chemiluminescence (ECL). SLG was used with classical ECL luminophores, rubrene, tris(2,2′-bypyridine)-ruthenium(II) and 9,10-diphenylanthracene in an inert environment to generate stable electrochemical responses and measure light emission through the material. SLG displayed excellent stability during electrochemical potential stepping and voltammetry in a window that spanned at least from -2.4 V to +1.8 V versus a QRE in acetonitrile and acetonitrile/benzene with sufficiently facile electron transfer properties to yield stable voltammetric cycling and ECL. SLG electrodes patterned with poly-tetrafluoroethylene permitted the stable generation of radical ions on an SLG microelectrode to be studied through Scanning Electrochemical Microscopy (SECM) in the generation/collection mode. The transparency of graphene was used to obtain accurate spectral responses in ECL: while inner filter effects are known to cause a shift in peak emission wavelength of spectroelectrochemical studies, the use of SLG electrodes with detection through the graphene window reduced apparent peak shifts by up to 10 nm in wavelength. This work introduces SLG as a transparent, electrochemically active and chemically stable platform for studying ECL reactivity in the radical annihilation mode, where large electrode polarizations could compromise the chemical stability of other existing transparent electrodes. Additionally, steady state radical annihilation ECL was explored via thin layer cells and SECM.

Acknowledgements

There are many people to thank for help over the past two and half years. Firstly, I would like to thank my advisor, Joaquin Rodriguez-Lopez, for teaching me more than I thought I could know. I would also like to thank Ryan Bailey for his support and guidance; Scott McClaren at MRL's AFM lab for both advice with research and conversation; Ellen Althouse for helpful discussions. Patricia Simpson and Julie Sides were sources of support for me throughout my time at the university; I am incredibly thankful for and appreciative of their advice, guidance and understanding.

I would like to extend my sincerest thanks to Drs. Toni Barstis, Chris Dunlap, and Dorothy Feigl at Saint Mary's College for their encouragement over the past six years. I cannot express in words how grateful I am for everything they have done for me.

Thank you to members of my group for teaching, collaborating and learning together. Beyond thanks for academic help I would like to thank Zack Barton and Burt Simpson for initiating me to Star Wars and Firefly; Mark Burgess and Michelle Colombo for a better understanding of the beginning of the universe; Jinghu Hui for delightful conversations; and Adam Chinderle and Tim Lichtenstein for listening to me rant and still being my friend.

Thank you to all of my friends both in and out of Urbana-Champaign. Your conversations, distractions, and love have made my time here more enjoyable than I thought possible.

Lastly, I would like to thank my family, especially my mom, for listening to me eventhough they do not know anything about chemistry.

Table of Contents

Chapter 1: Introduction to Graphene and Electrochemistry

We present the use of large area single layer graphene (SLG) electrodes obtained by chemical vapor deposition (CVD) as chemically stable and transparent platforms for electrochemical studies coupled with spectroscopic electrogenerated chemiluminescence (ECL) in non-aqueous media. SLG has garnered much interest for use in electronics, biosensors, and electrochemistry due to its unique electronic behavior and optical transparency.[1-6] CVD SLG can be prepared to yield electrodes of a few cm^2 and can be easily transferred to a variety of substrates, such as silicon and transparent materials such as glass. This method results in electrodes where the basal plane of SLG, as characterized via Raman spectroscopy, is exposed to species in solution. These atomically thin electrodes have been shown to readily engage in outer-sphere electron transfer, displaying slow electrochemical kinetics for certain redox mediators. Most work on graphene materials, however, has focused on exfoliated flakes of multilayer graphene or reduced graphene oxide,[7-9] which are produced through wet chemical methods. In order to obtain a conductive substrate multilayer deposits must be used which decreases the optical transparency whereas SLG is up to 98% transparent in visible region of light. In addition, structural and chemical defects created during the synthesis of exfoliated graphene flakes can significantly alter the electrochemcial activity, thus obscuring mechanistic studies of electrochemical light emission. Thus, it is of interest to evaluate SLG as a pristine electrode with high transparency for the generation of radical annihilation ECL.[3, 4, 10-13] Experiments with pristine SLG could lead to a better understanding of the role of defects and grain boundaries in the behavior of carbon materials.[6, 12-17]

Here, we will focus on the use of SLG in an electrochemical environment for the generation of

light through ECL.[18-32] ECL can be produced by two different modes: co-reactant or annihilation.[31, 32] Co-reactant ECL is typically conducted in aqueous solution and consists of a single potential step experiemnt where both the luminophore and a sacrificial co-reactant are simultaneously reacted at the electrode surface to produce emission. Previous work has shown use of graphene as a support for $Ru(bpy)_3^{2+}$ impregnated thin films to probe co-reactant ECL in an aqueous medium.[33] In the present work, we use pristine SLG to produce ECL *via* the annihilation mechanism, a schematic of which is shown in Figure 1.1. In this work, we demonstrate that large area graphene electrodes can be polarized to yield an electrochemical window as required for the generation of the radical ions in Figure 1.1. Despite the large polarization, we will show that SLG electrodes display stable electrochemical operation.

SLG readily engages in outer sphere electron transfer[5] while displaying lower activity for electrocatalytic transformations. [6, 12, 15]As an allotrope of carbon, SLG is sufficiently conductive to behave as an electrode, similar to boron doped diamond, glassy carbon and highly ordered pyrolitic graphite (HOPG), but offers an enchanted transparency.[17, 34-36] Graphene has been observed to perform both oxidations and reductions in aqueous solution,[5] however the potential window for aqueous electrochemistry is much smaller than that needed for radical ion annihilation ECL. Additionally, cobalt complexes have been adsorbed to the surface of graphene and used for electrochemical reactions.[15]

A transparent electrode is convenient for spectroelectrochemical experiments. Traditional ECL measurements are known to display shifts in their emission spectra when compared to photoluminescence (PL) spectra due to inner filter effects. Unlike PL, in ECL the light must pass

through a concentrated (~several millimolar) solution of the luminophore.[37] The use of a transparent electrode would allow radical annihilation ECL to be measured on the backside of the electrode. Transparent metal oxide electrodes, such as indium doped tin oxide (ITO) and fluorine doped tin oxide (FTO), are the current standard for transparent electrodes but they are mainly useful for oxidation chemistry as they become unstable upon reduction in organic media.[38, 39] Recent works explore thin films of carbon nanotubes and metal nanowires as transparent electrodes, but these materials quickly decrease in transmittance in order to increase conductivity.[40] These materials absorb at least 20% of the visible wavelengths of light when they are at their ideal maximum resistance, whereas SLG absorbs only 2% of visible light.[40]

Using Scanning Electrochemical Microscopy (SECM), we show that it is possible to produce radical ions at using graphene as a substrate both at steady-state and with high collection efficiency. Previous work utilizing radical annihilation ECL has observed steady-state emission from rubrene (RU) by using SECM[41] as well as single chemical reactions[42]. This work was limited by the use of ITO since it can only produce stably radical cations. We offer SLG as an alternative transparent electrode for electrochemical studies coupled with optical measurements. Since graphene is stable at both oxidizing and reducing potentials it is an interesting material for SECM studies and SECM/ECL coupled studies.[1, 41, 43, 44] We show that SLG maintains electrode behavior in a 4 V potential window producing both radical anions and radical cations. Although atomically thin, here we show that SLG's electronic conductivity and optical transparency make it an ideal platform for spectroelectrochemical experiments.

Another way in which SLG electrodes and SECM can be utilized is for the study of charge transfer inverse photoemission (CTRIPS). As a very simple definition, CTRIPS is an electrochemically induced light emission process from the electrode material rather than the solution.[45] Previous work has observed an emission thought to be CTRIPS via SECM by bias the substrate electrode such that radical cations are formed and slowly scanning the tip potential such that radical anions are formed.[41] While the ECL emission should correlate well to the tip current, i.e. the intensity of light produced is directly proportional to the amount of radical anions (cathodic current) produced. A pre-emission peak was observed which may be CTRIPS. The emission mechanism of CTRIPS is caused by hot charge carrier injection into a metal, relaxtion of that carrier, and emission of the relaxation energy.[45] The emission is mainly via thermal energy, but is also light. Since CTRIPS should occur before ECL the wavelength should be more red-shifted and therefore detectable via spectroscopic studies. This work attempted these measurements via transient ECL experiments but the results did not indicate any emission besides ECL.

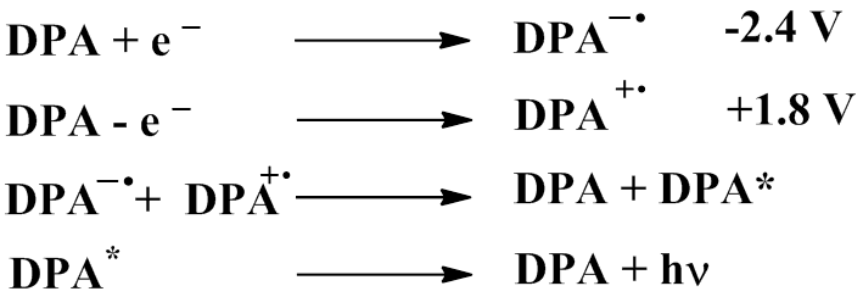

Figure 1.1: Radical annihilation ECL of a generic mediator R. Last step shows emission of photon of energy hν

Chapter 2: Materials and Methods

2.1 Chemicals

Rubrene (≥98%), electrochemical grade supporting electrolyte tetra-*n*-butylammonium hexafluorophosphate ($TBA.PF_6$), and anhydrous acetonitrile (99.93%) were obtained from Sigma-Aldrich Co. (St. Louis, MO) and used as received. 9,10-Diphenylanthracene (DPA, 99%) was purchased from Aldrich (Milwaukee, WI) and twice recrystallized with xylenes before use. Benzene was purified by passage through a bed of activated alumina immediately prior to use (Glass Countour, Laguna Beach, California).

Most chemicals in the lab needed to be purified before use. Chemicals ordered from Sigma-Aldrich must be at least 99% pure and anhydrous. DPA (Aldrich) must be recrystallized in xylenes, usually at least twice. During the recrystallization a hot filtration should be carried out to remove impurities. This is simply a gravity filtration while the solvent/DPA mixture is hot (i.e. DPA is dissolved). DPA may precipitate on the filter paper, which can simply be addressed by rinsing with hot xylenes. The filtered solution should be returned to the hot plate for a few more minutes to remove some of the solvent. The flask should be removed from the heat and submerged in an ice bath to induce the DPA to precipitate from the solution. The crystals should then be collected via vacuum filtration. DPA should be twice recrystallized and dried overnight in a vacuum oven at 100 °C before use. The purified DPA should be stored in an inert environment.

Several $Ru(bpy)_3^{2+}$ salts were made via a metathesis reaction. $Ru(bpy)_3Cl_2$ was dissolved in a minimal volume of water while in a separate container an ammonium or potassium salt of the

Sample preparation and characterization was carried out in part in the Frederick Seitz Materials Research Laboratory Central Facilities and the Micro and Nanotechnology Laboratory, University of Illinois.

desired anion is similarly dissolved. The two solutions are combined to form ammonium chloride and a $Ru(bpy)_3^{2+}$ salt with an organic anion (e.g. hexafluorophosphate, $BArF_{20}$).

2.2 Graphene Preparation

Glass supports for SLG electrodes were fabricated from glass slides cut into ~1 inch wide samples. Prior to being cut to size the samples were coated in gold via electron beam evaporation so that strong electrical connections could be made to the SLG, as shown in Figure 2.1.

SLG was grown by chemical vapor deposition on Cu foil (25 μm, Alfa Aesar).[11] The copper foil were treated with acetone (10 s), water (DI) (10 s), glacial acetic acid (Fischer Scientific, 10 min), water (DI) (10 s), acetone (10 s), and isopropyl alcohol (10 s) before growth. The Cu foil was then loaded into a quartz tube in a tube furnace. Hydrogen was flowed at 500 sccm as well as Argon was flowed at 1000 sccm for 5 minutes. The system was pumped 40 mTorr of pressure, then hydrogen was flowed at 50 sccm for the remainder of the growth and Argon was flowed at 1000 sccm until eaching the growth temperature. The system was then heated at 1000 °C and graphene was grown under the flow of 100 sccm of CH_4 for 65 minutes. The system returned to room temperature and pressure while 500 sccm of Argon was flowed. A layer of poly(methyl methacrylate) (PMMA) was added for support during transfer. 495 PMMA A2 (MicroChem) was first spin coated on top of the graphene at 3000 rpm for 60 s. Two layers of 950 PMMA A4 (MicroChem) were then spin coated at 3000 rpm for 60 s.

Copper etchant solution (Transene Company, CE-100) was used to remove the copper from beneath the graphene/PMMA. The graphene/PMMA was then transferred to water and washed

three times to rinse away the etchant salts. The graphene/PMMA was then transferred to 0.1 M EDTA (Fischer, 99%) for 1 h. The graphene/PMMA was then transferred to water and washed three times to rinse away any remaining chelating agent. The graphene/PMMA was then transferred onto a piece of glass slide that was half coated in gold to make a good electrical contact and blown with argon to dry. To remove the PMMA, the sample was placed in anisole for 3 h, then placed in a dichloromethane/acetone mixture (1:1) for 5 h and finally placed in isopropyl alcohol for 2 h. The sample was then blown with argon to dry.

To form SLG microelectrodes as well as a barrier between the SLG and the o-ring of the electrochemical a protective layer of polytetrafluoroethylene (PTFE) was selectively deposited on the surface in accordance with an existing method.[46] Briefly, a positive photoresist was deposited onto the substrate with a micropipetter (<1 μL) and allowed to dry. A PTFE precursor was loaded onto the substrate via spin coating. Once dry the sample was shaken in acetone to remove the photoresist, leaving pores in the PTFE where the photoresist was. The PTFE was cured in a furnace under an inert atmosphere at 350 °C for 20 minutes. The resulting PTFE coated sample is shown in Figure 2.2.

Raman spectra of SLG samples were collected with a Nanophoton Raman-11 laser Raman microscope using a 532 nm laser. Atomic force microscopy (AFM) analysis was performed on an Asylum Cypher AFM using silicon cantilevers coated in aluminum in tapping mode.

2.3 Electrochemical measurements

Electrochemical experiments were performed in an inert environment using a CHI1242b portable

bipotentiostat (CH Instruments, Austin, Texas). Solutions were prepared in an argon atmosphere glovebox. Cyclic voltammograms (CVs) were obtained using a silver wire as a quasi-reference electrode (QRE) and a platinum wire as a counter electrode. All potentials are reported versus the QRE unless otherwise stated. The CVs showed at which potentials the radical cations (E_{ox}) and anions (E_{red}) were generated. Chronoamperometry was used to step between E_{ox} and E_{red} to produce radical annhilation ECL.

2.4 SECM measurements

A 50 μm radius gold electrode was prepared by sealing a gold wire (Goodfellow) in a 1.5 mm outer diameter and 0.75 mm inner diameter patch clamp glass capillary (World Precision Instruments) using a heated metal coil. Electrical connections were made to the gold wire filling the unsealed portion of the capillary with silver epoxy (Ted Pella) and inserting a long wire before curing the epoxy. The gold was exposed and the electrode sharpened to a tip by manual grinding.

Figure 2.1 depicts the confiuration used for radical ion collection experiments using SECM. The gold tip was biased to E_{red} and approached to the PTFE coated region of the substrate in feedback mode, displaying a decrease in current as it approached the insulating PTFE (i.e. negative feedback). Then the tip was then scanned across the sample using the tip generation/substrate collection mode in order to find a graphene microelectrode. When a spot of exposed SLG was found, the tip was aligned above that spot and approached with the substrate biased at 0 V to collect the radical anion from the tip. Tip generation/substrate collection experiments were performed where a radical ion is produced at the tip and then converted to its original oxidation

state by the substrate. To calculate collection efficiency a tip generation/substrate collection CV was obtained with the tip directly above the exposed spot of graphene.

2.5 ECL and Fluorescence Measurements.

To produce transient ECL, the electrode potential was stepped between an oxidizing (E_{ox}) and reducing potential (E_{red}) every 0.5 seconds. Spectroscopic data was collected with the different configurations depicted in Figure 2.2. Configuration A was used with the commercial polymer-encased metal electrodes (Au and Pt), where the electrode was suspended in solution such that the ECL could be collected by a fiber optic placed below the glass base. Light had to traverse several mm of solution to finally exit through the glass base. Configurations B and C correspond to measures with a SLG electrode. The first case served as a control experiment to evaluate inner filter effects. In this case, light generated via ECL close to the surface of the SLG electrode had to travel though several mm of solution to be collected at the fiber optic. In configuration C, ECL was collected as it directly went through the transparent SLG electrode with the fiber optic placed beneath the base. In all cases, the collected light on the fiber optic led to a CCD spectrometer (Avantes, AvaSpec-ULS3648TEC). Spectra were collected with the shutter open for 40 seconds and averaged 10 times. PL emission spectra were collected with dilute solutions of RU in benzene and DPA in acetonitrile using a Cary Eclipse fluorometer.

2.6 Stepping Experiments for CTRIPS

First attempts to obtain spectra of ECL emission were labor intensive. The cell could be assembled in multiple ways. One way was to use a piece of Si wafer with either gold or platinum deposited on the surface. This was then put into an SECM cell with the fiber optic directly above

the cell. Alternatively, a long, thin piece of metal was placed in a cuvette with a counter electrode behind it facing away from the fiber optic. ECL was produced via chronoamperometry. The fiber optic was directed at the working electrode in the cell and lead to a monochromator. The monochromator was set to make 5 nm steps every 2 seconds with a PMT on the output for detection. This data was then analyzed in MS Excel by integrating the data every 2.5 seconds via trapezoid integration. This accounts for the time it takes the monochromator to change wavelengths and to average the signal due to its transient nature.

The potentials were stepped between an E_{ox} at an overpotential of 70 mV and a variable E_{red}. Full spectra were collected with E_{red} ranging from an underpotential of 150 mV to an overpotential of 100 mV. This covered the potential window in which a pre-emission peak was observed using a solution of rubrene, an ITO substrate electrode and gold tip via steady state radical ion annihilation ECL experiments using SECM.The reduction potential used varied by 20 mV at the onset of the electrochemical reduction peak, but larger steps were taken when higher potentials were reached.

2.7 Thin layer Cell

A thin layer cell configuration was attempted in order to produce steady state ECL on a large scale. A piece of fluorine doped tin oxide (FTO) was sandwiched with a piece of glass with 2 separate stripes of gold. A layer of Teflon tape was used as a spacer between the electrodes. Several different configurations were attempted. FTO must *never be taken to reducing potentials* or else it will degrade and contaminate the solution. After working with Teflon tape the experiments were repeated with PDMS as the spacer and a metal clamp to keep the electrodes as

close as possible without touching. PDMS was spin coated onto various surfaces (petri dish, Si wafer, glass) before being cured at a thickness of 500 nm. Examples of both Teflon tape and PDMS thin cells are shown in Figure 2.3. Large area electrodes were used in an attempt to observe steady state radical ion annihilation ECL and CTRIPS on a scale visible by eye and easier to detect for quantification.

2.7.1 Traditional two-electrode system:

A two electrode system was attempted with FTO at an oxidizing potential and gold as the alternate electrode.

2.7.2 Modified two-electrode system

One gold stripe was used as a shorted out counter/reference electrode. The FTO was held at E_{ox} and the second gold stripe was scanned via cyclic voltammetry across E_{red}.

2.7.3 Three electrode system

A silver wire was included in the solution as a quasi-reference electrode. One gold stripe was used as a counter electrode and one was used to obtain a CV of the reduction of the mediator. The FTO was held at Eox.

2.8 Transient ECL Measurements

Transient ECL measurements were performed with a photomultiplier tube (PMT). Initially an older (Oriel) PMT was use and connected to a high voltage power supply (Oriel detection 7070). The PMT was biased to 750 V during measurements.

The newer Hamamatsu PMT is sufficient for transient measurements with large (>250 μm radius) electrodes can be obtained without filtering the signal output from the PMT. Measurements of small quantities of light she be collected with a low pass filter between the signal output of the PMT and DAQ. This removes most environmental noise from the signal. Without this filter there are several spikes in the signal up to 100s of mV that disrupt the signal. Whenever possible, however, measurements should be repeated without the low pass filter to compare and to be sure that it is necessary. This is because the filter can distort the peak shapes and even block some of the smaller intensity signals from being sent to the DAQ. A diagram of how the Hamamatsu PMT should be connected to the power supply is shown in Figure 2. 5.

2.9 Electrodeposition of nanoparticles

All work for the electrodeposition with nanoparticles was done with a Pt counter electrode and bridged Ag/AgCl reference electrode. It is herein advised that work with gold nanoparticles be completed with a gold counter electrode to reduce the risk of contamination with platinum.

A solution of 3 mM chloroplatanic acid (H_2PtCl_6) in 0.5 M sulfuric acid (H_2SO_4) was used for the growth of Pt nanoparticles. Nanoparticles were grown by cycling 25 times between -0.25 V to +0.65 V versus a Ag/AgCl reference electrode at 50 mV/s.[47] This should yield 500 nm particles or clusters of smaller particles. Hydrogen evolution reaction (HER) was used to confirm the presence of Pt on the graphene samples with a 0.1 M solution of H2SO4 by first scanning samples of pristine SLG and then repeating the same cyclic voltammagram on SLG decorated with Pt nanoparticles.

To grow gold nanoparticles, 0.5 mM chloroauric acid ($HAuCl_4$) was dissolved in 0.1 M H_2SO_4.[48] To nucleate gold nanoparticles the graphene electrode was held at -239 mV for 0.1 seconds, immediately followed by 25 seconds at +886 mV versus a Ag/AgCl reference electrode. To confirm the presence of gold on SLG samples lead under potential deposition (UPD) was used. This simply electrochemically deposited a film of lead at an underpotential such that it will only deposit onto gold, a known phenomenon, and then via anodic stripping the lead is removed.

Scanning electron microscopy (SEM) with energy dispersive X-ray spectroscopy (EDX) was initially used to analyze samples of graphene and HOPG decorate with nanoparticles using a Hitachi 4700 High Resolution SEM. Nanoparticles of gold, copper, and gold/copper, provided by Paramaconi Rodriguez at the University of Birmingham, were obtained to deposit onto the graphene samples, but this was never done.

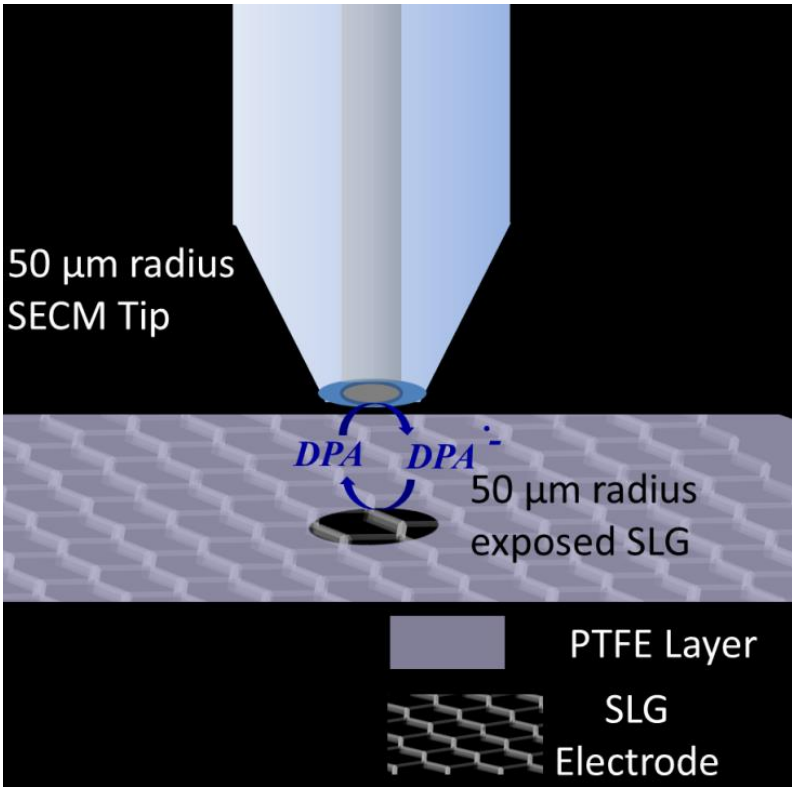

Figure 2.1: General layout of SECM tip aligned above a hole in the insulating PTFE layer allowing interaction solely between the tip and the single spot of SLG.

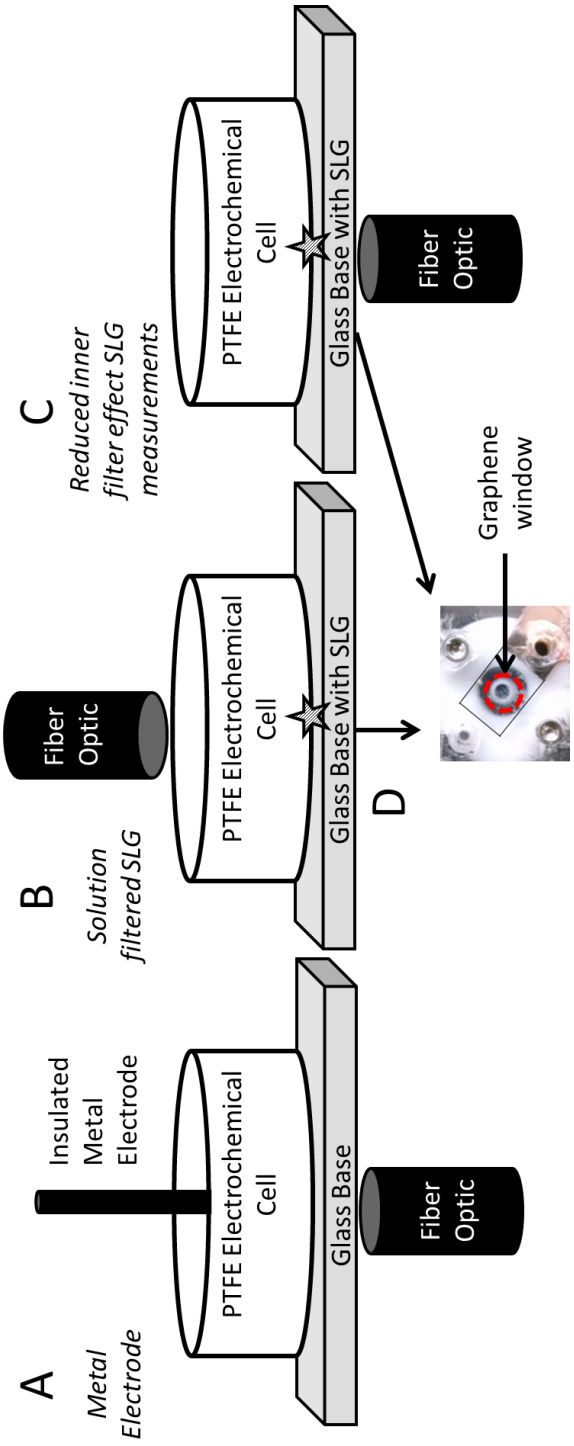

Figure 2.2: Experimental design for ECL spectroscopic measurements with a metal electrode surrounded by an insulating sheath (A), a SLG electrode with the fiber optic cable positioned such that the light must pass through the solution before collection (B), and a SLG electrode with the light measured beneath the cell (C). The base of a typical cell used is shown in (D) where the area within the red dashed line is the only region exposed to the solution. In (B) and (C) the presence of SLG is represented by a star.

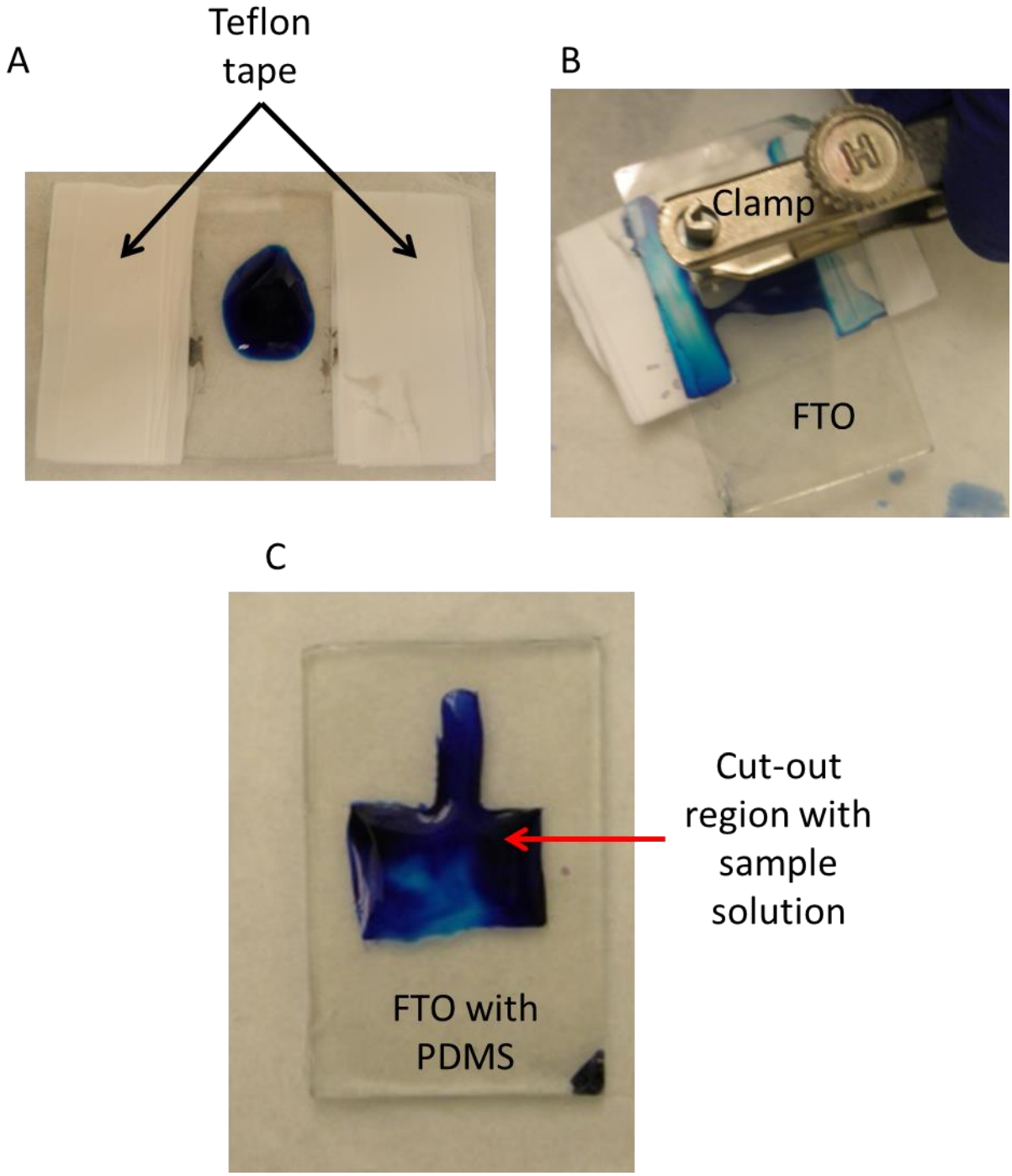

Figure 2.3: Sample configurations for thin cell studies with a blue dye for clarity. In A and B teflon tape is used as a spacer between electrodes and then the plates are clamped together, however this caused the solution to quickly escape the set up. The configuration in C used PDMS as a spacer which did not stick well to FTO, but was better than teflon tape.

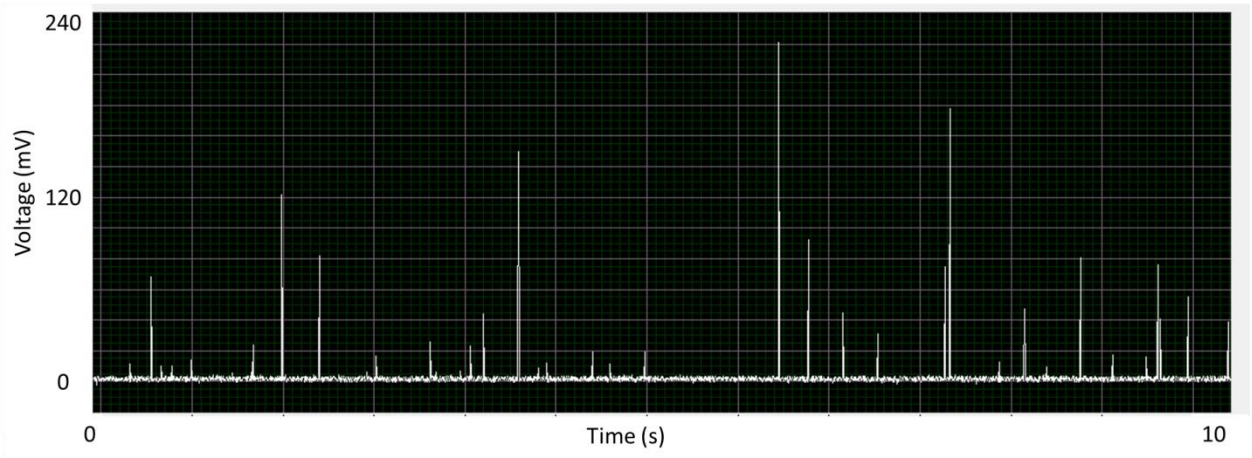

Figure 2.4: Dark current measurements using the Hamamatsu PMT showing the need for a low pass filter

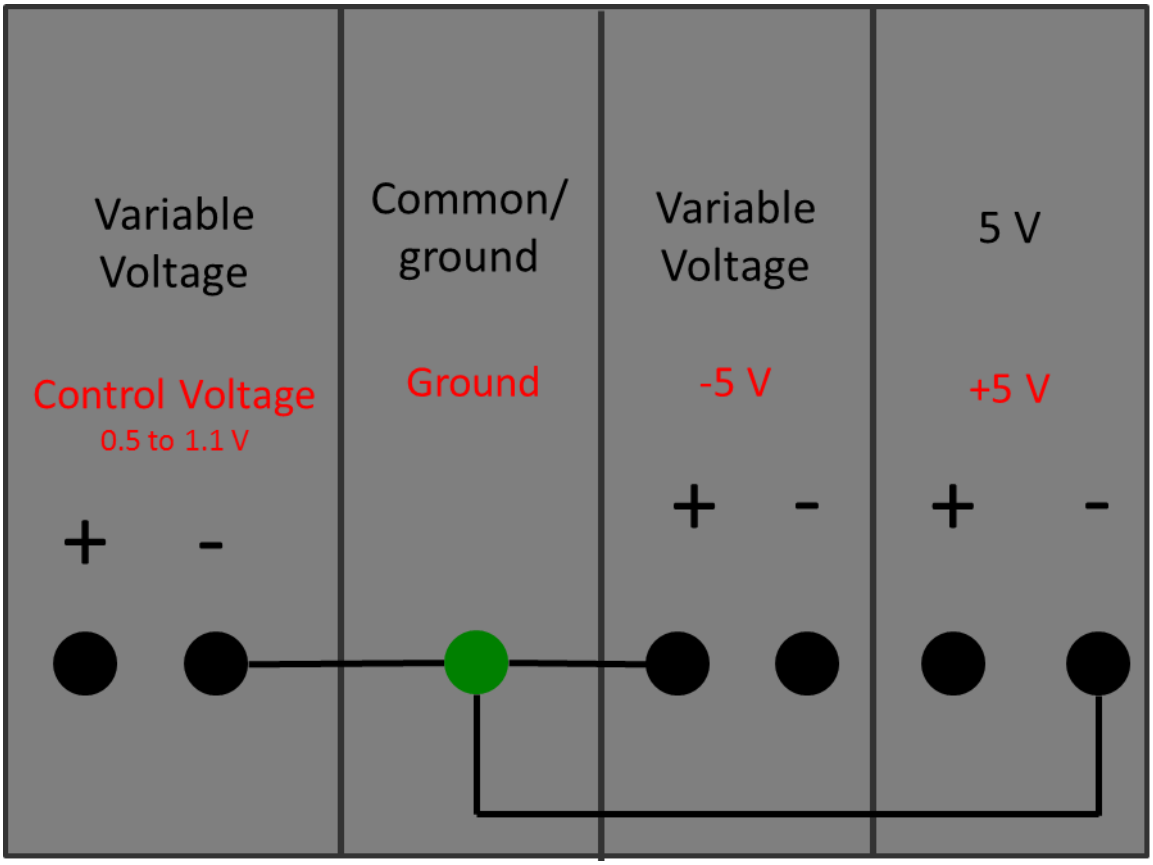

Figure 2.5: Electrical configuration for connections between the power supply and Hamamatsu PMT

Chapter 3: Steady State Radical Annihilation ECL

3.1 Initial Work

Most initial work focused on refining experimental technique and materials. This began with co-reactant ECL which can be obtained with $Ru(bpy)_3^{2+}$ and sodium oxalate in phosphate buffered saline (PBS). While co-reactant ECL was not utilized in this work it is very useful to understand this as a starting point for radical annihilation ECL and to be used in outreach activities.

Purification of chemicals was necessary at the onset of this work, however it later became apparent that purchasing higher-grade reagents was more efficient. Recrystallization of DPA was an exception as it was carried it in relatively large quantities (~1 gram at a time) and the resulting compound stayed pure when stored in an inert environment. Benzene, for work with RU, worked best when obtained from the solvent distillation system in the White lab immediately before use. Various salts of $Ru(bpy)_3^{2+}$ were successfully synthesized, but rarely used as they never purified to the degree necessary to produce ECL. The most likely issue here was trace amounts of water still present in the salts.

3.2 Stepping Experiments for CTRIPS

At approximately 100 mV before E_{red} an emission peak was observed, followed by an increase in intensity when ECL should begin. These stepped ECL experiments were attempting to observe a red-shifted emission that would correspond to the pre-emission peak. Initial results saw a peak of green emission when using a SLG electrode to excite DPA (a blue emitter), however this was quickly shown to be a contamination from Pyrromethene 567a (a BODIPY dye). Other than this no emission peaks other than those correlating to PL were observed with any electrode material

or luminophore. Transient experiments are not likely to be useful for studies of CTRIPS as no pre-emission was ever observed. That being said, it would be advisable to repeat the stepping experiments with rubrene and gold with a more sensitive spectrometer.

3.3 Thin Cell

All forms of the thin cell were unsuccessful at producing steady state radical annihilation ECL. Theoretically, this should have been possible and would be a superior way to probe CTRIPS as the light would easily be detected. Unfortunately, this set up is difficult and time consuming. With the proper knowledge of and access to microfluidics this should be an entirely feasible experiment. However, metal oxide electrodes should be avoided at all costs in radical annihilation ECL experiments. SLG is a far superior option as it can be transferred to a variety of materials, is more optically transparent, and can be used in a large potential window, as will be shown in the following chapter.

3.4 PMT

Unfortunately, the Oriel detector was not sensitive enough to detect microelectrodes and the recovery time was too slow to detect fast pulses. Figure 3.3 shows the transient emission from $Ru(bpy)_3^{2+}$ using a large platinum electrode. Every other electrode pulse has a decreased ECL signal, likely due to the detector recovering from the previous pulse.

The Hamamatsu PMT should be sufficient for most measurements when used with a Kiethley DAQ. The National Instrument DAQ should not be used for ECL measurements as it cannot read signals quickly enough.

3.5 Electrodeposition of nanoparticles

Pt on HOPG was observed via SEM prior to access to EDX, shown in Figure 3.4. Unfortunately the particles were mostly larger than the nano-scale. The most likely explanation is that the particles are nucleated on the first step and then grow during the second pulse, but begin to aggregate. The electron beam in the SEM may also contribute to aggregation. Furthermore, SEM is not a practical tool for graphene analysis as the sample is mostly glass and charge builds up quickly. This prevents a sharp image from being captured and damages the graphene.

EDX is also not suitable for graphene samples. The main elements detected are those present in the substrate (glass slide, in this case) rather than carbon (graphene) or gold (nanoparticles). After aid from SEM staff carbon was observed via EDX, but with low intensity. Exemplary results are shown in Figure 3.5

It is not clear whether or not nanoparticles ever grew from SLG. For future studies it would be interesting to study nanoparticles that grew directly onto the SLG, but it may not be worth the time to refine a method to do so. Work with HER and lead UPD was mostly done in preliminary stages to confirm that the techniques could be used rather than actually being used experimentally. SLG samples at this early stage did not usually last long enough to do all of the experiments before the connection was damaged and trace lead remained in the cell after vigorous rinsing this making it impossible to use those samples for ECL studies. This basically renders the work useless as the nanoparticles needed to be grown, confirmed to be there and then used in an SECM experiment. Deposition of already formed nanoparticles may prove to be equally interesting, especially those produced via cathodic corrosion due to the lack of

surfactant. It may, however, be advisable to synthesize the nanoparticles immediately before deposition to reduce any chance of aggregation in solution, as is highly likely since the particles have no capping agent.

3.6 Substrate preparation for SLG electrodes

While it is difficult to quantify the effect these steps had on the performance on SLG electrodes, it is anecdotally supported. Previous to using gold contacts measurements with SLG electrodes were high in resistance, most likely caused by a poor electrical contact. The PTFE provided a barrier between the SLG and the o-ring of the SECM cell such that when the cell is tightened any structural damage is sustained by the PTFE rather than the graphene. This allowed graphene samples in an SECM cell to be re-used in similar experiments for up to a week. It is important that the cell only be re-used in similar experiments to avoid cross contamination between mediators. Nano- and μM concentrations of an ECL luminophore are sufficient to contaminate an experiment.

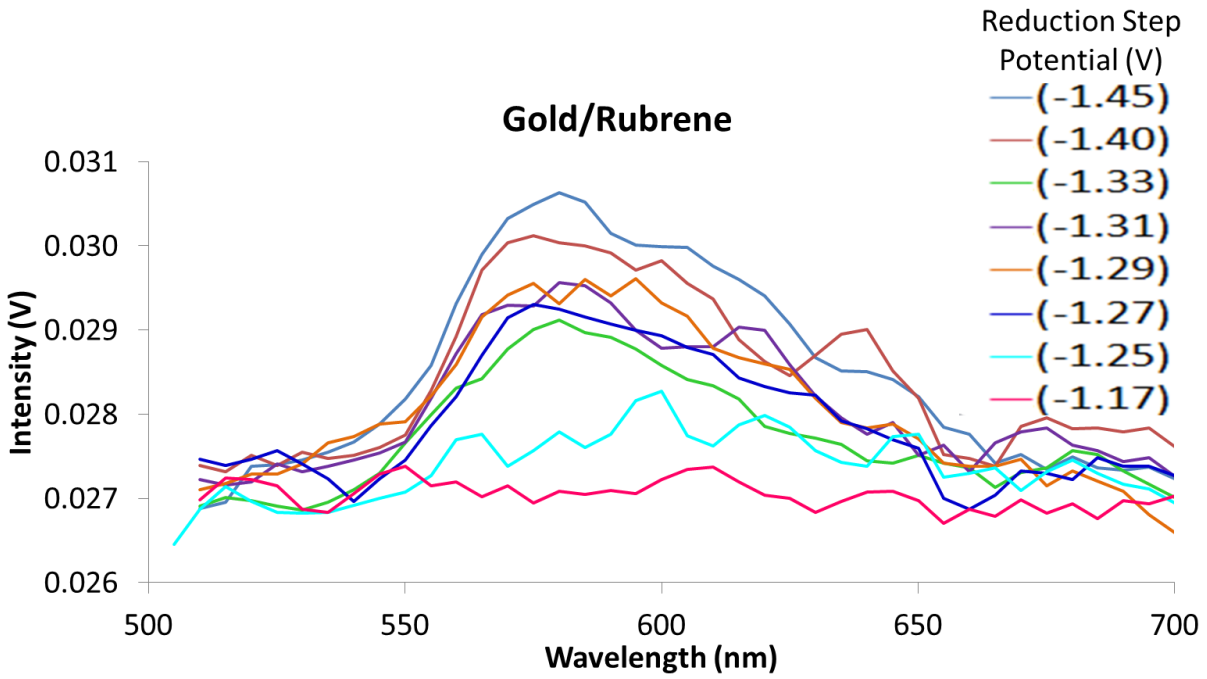

Figure 3.1: Spectra collected in CTRIPs stepping experiments using a large gold electrode and a solution of rubrene. For all spectra the electrode was stepped between +1.2 V (an 80 mV overpotential for the E_{ox}) and variations of the reduction potential ranging from -1.17 V to -1.45 V, all versus a silver wire, where E_{red} = -1.36 V.

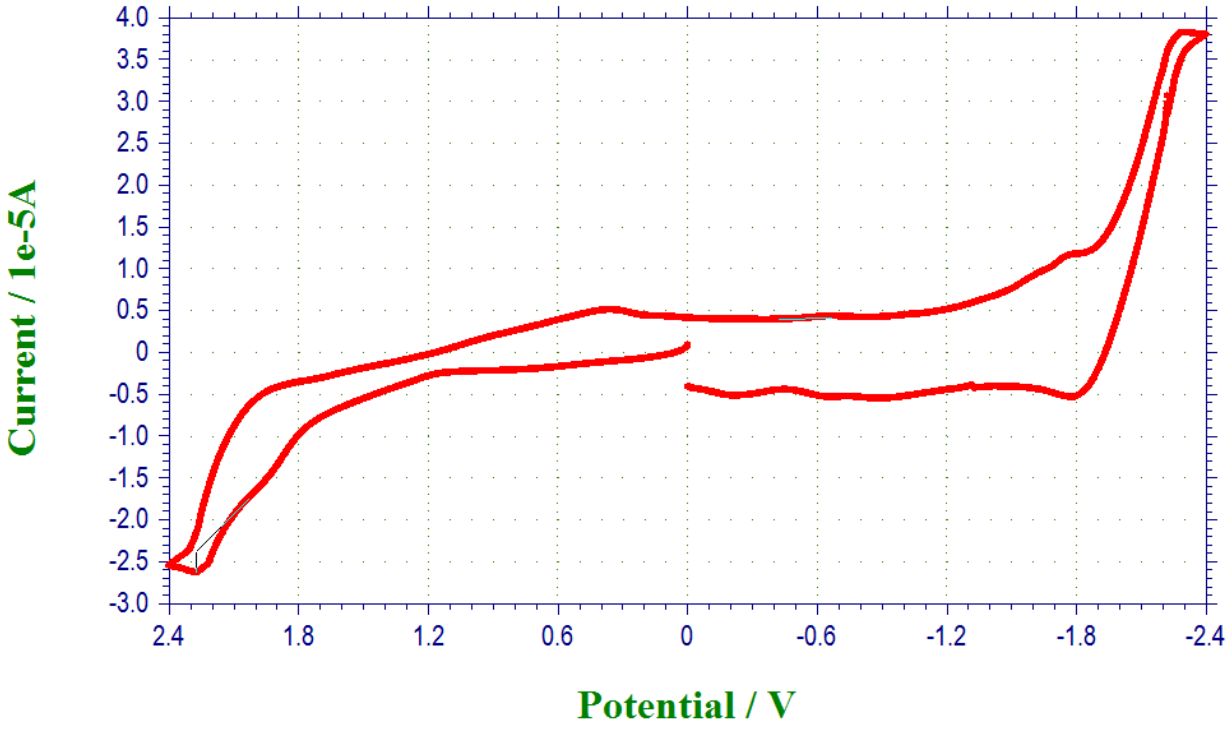

Figure 3.2: CV of Pyrromethene 567a in PDMS thin Cell using a gold working electrode, FTO substrate electrode and a shorted out gold CE/RE (the modified two-electrode system in section 2.7.2)

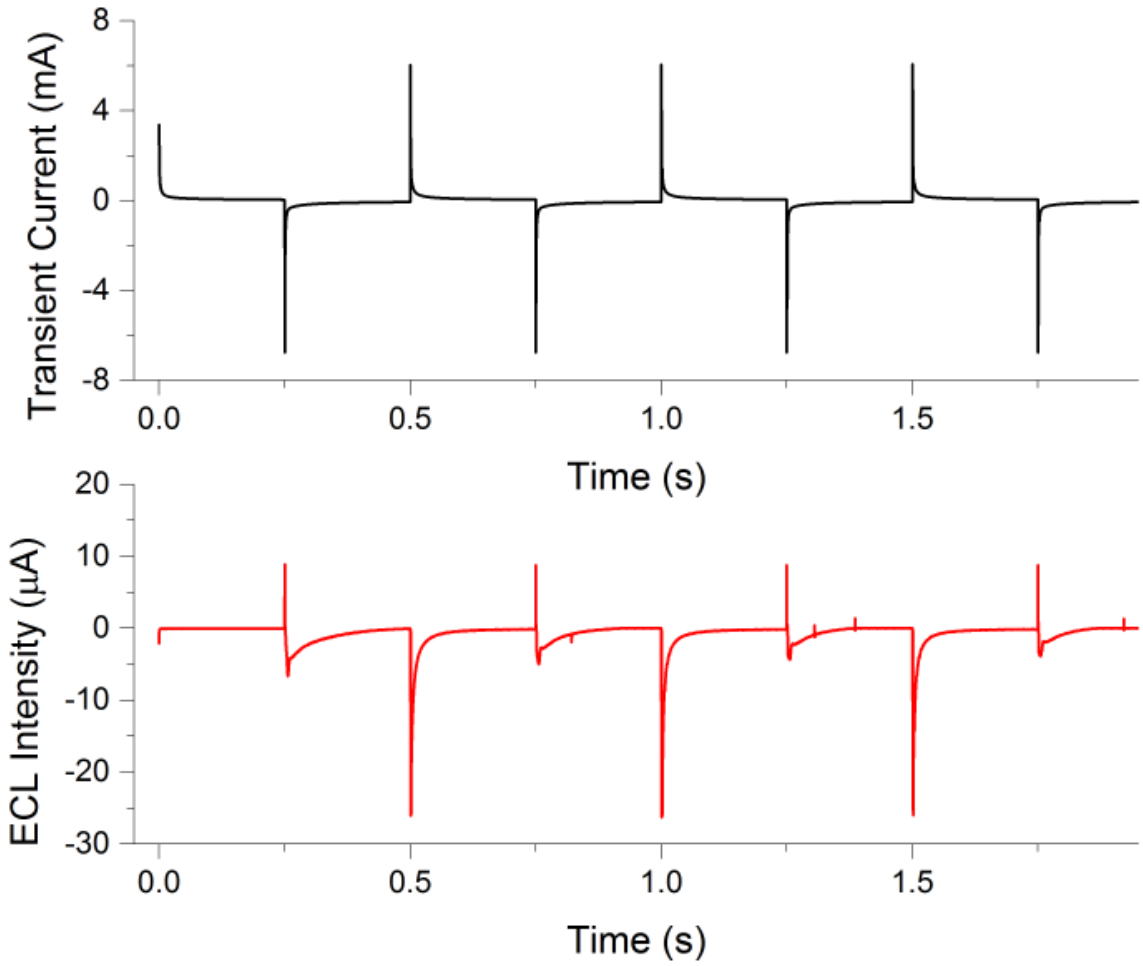

Figure 3.3: Transient current response from a platium electrode producing radical annihilation ECL of Ru(bpy)32+ (top) and the response of the Oriel PMT (bottom). The PMT reponse shows diminished ECL intensity every other pulse which is indicative of the recovery time of the instrument being too slow for these studies.

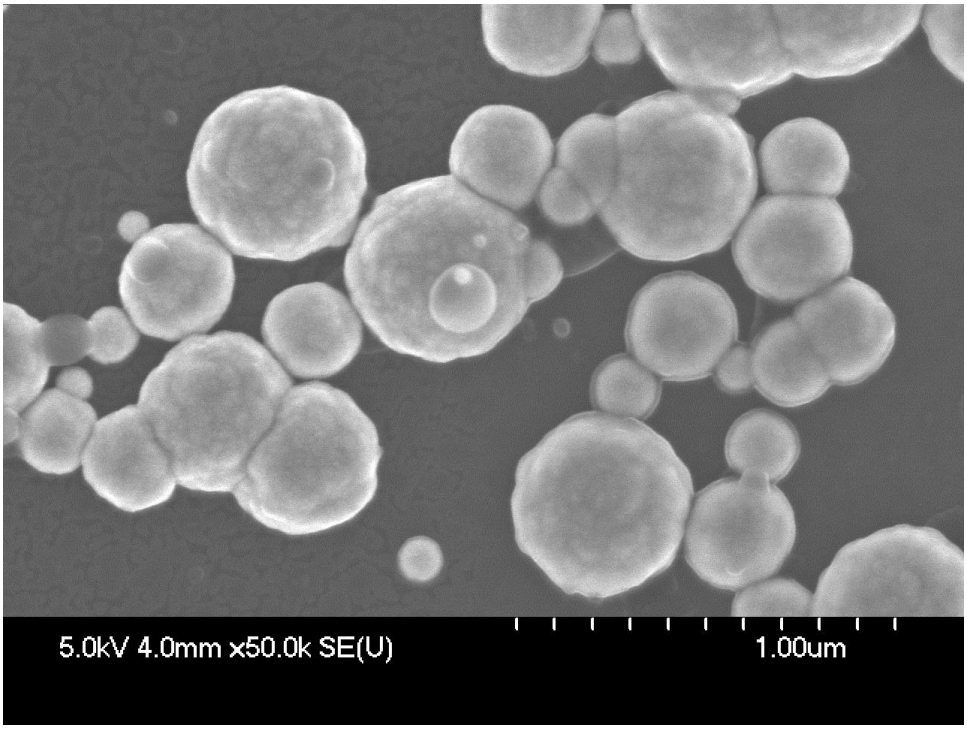

Figure 3.4: SEM image of HOPG after electrodeposition of platinum nanoparticles. The particles should have been ~500 nm in diameter but seem to have aggregated to even larger

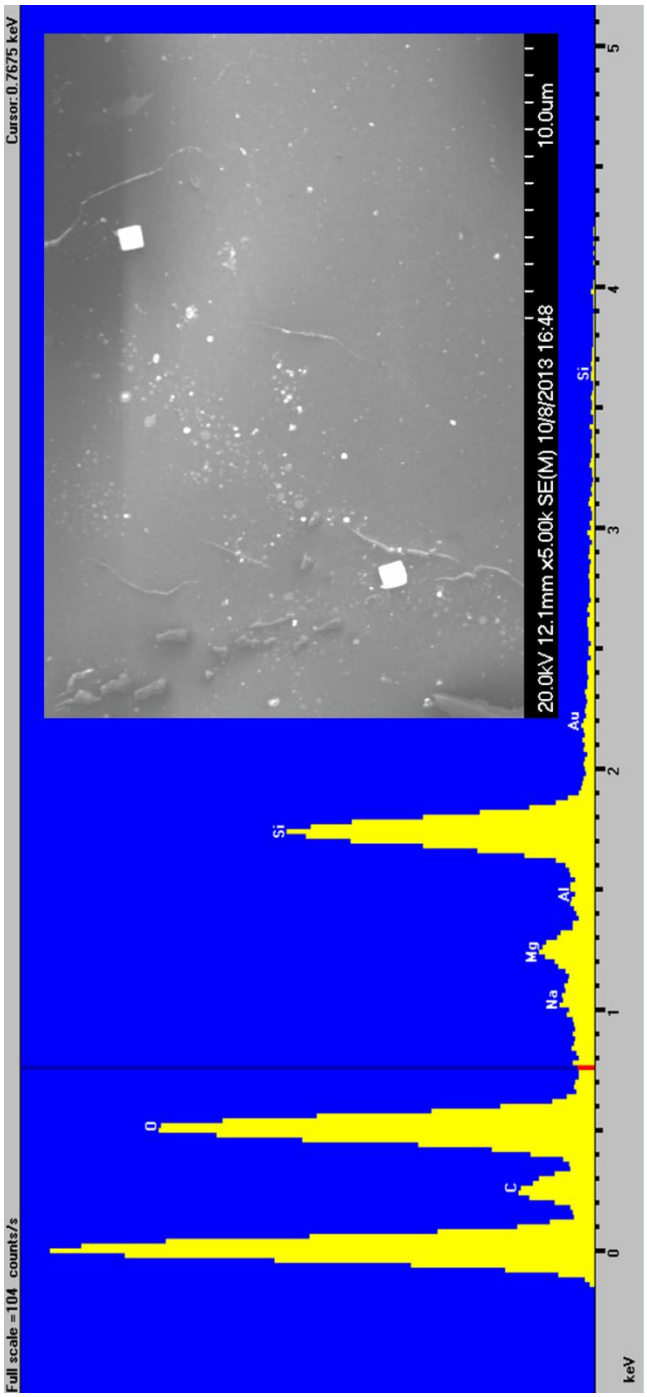

Figure 3.5: SEM image and EDX results of gold nanoparticles grown on SLG electrodes. The image shows some spots that may be nanoparticles but the EDX results do not show gold and in fact show more glass than anything else.

Chapter 4: Radical Annihilation ECL with Graphene Electrodes

4.1 Characterization of SLG.

Raman spectroscopy and AFM were used to assess the quality of SLG samples and are shown in Figure 4.1. A typical Raman spectrum of the SLG samples on Si/SiO_2 shows that the ratio of the 2D band at 2698 cm^{-1} to the G band at 1581 cm^{-1} is greater than two, indicating that the graphene was a single layer. A small D band at 1347 cm^{-1} suggest few defects on the SLG lattice. AFM shows a mostly smooth surface with several small (<10 nm) spots. Since the images were collect under ambient conditions some roughness may be attributed to dust. Additionally, SLG samples were on a glass slide without any corrections for roughness. Deviations in height may also be caused by wrinkles formed during the wet transfer procedure and from grain boundaries. Nonetheless, in general the quality of SLG samples was adequate for photoelectrochemical experiments.

4.2 SLG behavior as an electrode in large potential windows.

The voltammagram of DPA using a SLG electrode is shown in Figure 4.2 and shows the generation of the DPA radical cation (oxidation) and the generation of the DPA radical anion (reduction) in a 4 V window in acetonitrile from -2.4 V to +1.8 V versus a QRE. The different between the $E_{1/2}$ values is consistent with previously reported data for DPA, 3.4 V.[49, 50] SLG is suitable to use in non-aqueous media and can perform both oxidations and reductions without electrode degradation. The area calculated via the Randles–Sevcik equation using the parameters in Figure 4.2 is equal to 0.32 cm^2; this value is consistent with the geometric area of the electrode, 0.28 cm^2, which was exposed to the solution of DPA (Figure 4.2). This measurement ensures that the totality of the SLG was electroactive, and, as will be shown in the section

pertaining to ECL, that the entire electrode surface generated light. Once properly assembled into the electrochemical cell, the SLG electrodes could be re-used for several experiments under similar conditions as those in Figure 4.2, provided that the electrode is treated with care. For example, the sample of SLG used in Figure 4.2 was used in four experiments in an interval of a week before the cell was disassembled.

Table 4.1 shows the potential distance between the forward and reverse sweeps for CVs collected at both gold and SLG electrodes for RU and DPA. There is up to two times more peak splitting with the SLG electrode as compared to gold at 25 mV/s. Previous work has noted that graphene with electrochemically induced defects has shown more facile kinetic behavior than pristine graphene,[12] however, the presence of grain boundaries on large-area SLG grown through CVD method could also introduce resistance in plane current flow. The AFM image in Figure 4.1 shows evidence of these grain boundaries, therefore we explored the possibility that resistive drop could be dominating the peak splitting observed in Figure 4.2. The effects of solution resistance were incorporated into electrochemical simulations using commercial software (DigiElch 7). Despite this slight shortcoming in the experimental voltammetry peak splitting, SLG electrodes can engage in sufficiently facile electron transfer to the species in solution to generate radical ions for ECL. This is supported by SECM measurements of the collection of radical ions produced at the diffusion layer, as well as by the production of annihilation ECL, as shown in the following sections.

4.3 SECM collection measurements.

A sample of single layer graphene was selectively covered by a layer of (PTFE) and fabricated

to expose a small (hundreds of μm) active graphene microelectrode. This microelectrode was further addressed and imaged using SECM techniques. Figure 4.3A shows an approach curve done on the insulating PTFE layer using the reduction of diphenylanthracene as the mediated reaction. The approach curve fit will with theory[51] and showed a final tip-to-substrate distance of 10 μm with an electrode RG of 5 assuming total negative feedback. As observed for other carbons[46], PTFE makes an excellent protective layer and can be successfully microfabricated onto SLG Figure 4.3 shows a CV collected with the tip aligned above the region of exposed SLG held at a constant collection potential of 0 V vs. Ag QRE. At this potential, both the oxidation of the mono-radical anion and the reduction of the mono-radical cation to regenerate the parent DPA molecule were possible. SLG's collection efficiency for these radical ions was 92% and 60% for the reduced and oxidized species respectively. The lower collection efficiency of the radical cation compared to the anion suggests the presence of a scavenging species. A likely candidate would be traces of water in our setup. Nevertheless, this experiment shows that radical ion generation can be performed on graphene at steady state without compromising its stability in a reasonable time frame. Figures 4.3 C and D show SECM images of the micro-graphene spot, collected with the substrate at 0 V vs. Ag QRE. The SECM images show a small but highly electroactive by the insulating PTFE film, thus exposing an area of positive feedback (Figure 4.3C, tip current). This is more apparent in a plot of the collected radical ion by the SLG microelectrode (Figure 4.3D). During these experiments we did not observe any evidence of a decrease in activity of the graphene electrode, even after imaging and measurements during hours of operation. These images demonstrate that graphene is active as an electrode material in non-aqueous systems and that PTFE acts as a suitable protective layer that allows high-quality collection experiments to be performed.

4.4 ECL spectra of emission produced with a SLG electrode.

Radical annihilation ECL was produced via double-pulse chronoamperometry using electrode potentials where the radical anion and the radical cation where generated on alternate steps, as shown in Figure 1.1. Here, we used the classic luminophores DPA (blue emitter) and RU (orange emitter). In all cases the light was visible by eye in a well shielded dark room. The emission spectra are shown with the spectra in Figure 4.4A (DPA) and Figure 4.5A (RU). Figure 4.4C and Figure 4.5C show pictures of the emission on the transparent graphene electrode with contrast increased for clarity. These images reveal that the entire area delimited by the SLG electrode window in the electrochemical cell produce ECL, in accordance with the electroactive area estimated above. Figure 4.4E shows the transient decay of the ECL intensity over a single half-second pulse of the chronoamperometric measurement.

ECL emission on SLG electrodes shows a closer agreement to fluorescence in comparison to Pt and Au electrodes. Figures 4.4 and 4.5 show that the emission spectrum for the ECL on graphene and other electrodes is consistent with the fluorescence of RU and DPA. However, a more detailed analysis of the peak positions for the ECL and fluorescence are shown in the insets of Figures 4.4 and 4.5 and in Table 4.2, where we show the peak shifts of the ECL signals with +respect to those observed in fluorescence. On opaque metal electrodes where the ECL emission is measured *through the bulk of the solution*, there is a significant deviation of the emission peaks towards longer wavelengths with respect to PL. This is observed to be significantly smaller on graphene electrodes. For instance, the peak emission wavelength of RU is shifted for gold and platinum by 10 nm compared to fluorescence, while the emission produced by SLG,

which is measured *through the transparent graphene electrode* and not through the solution, is only shifted by 1 nm. Although peak shifts are much less evident for DPA than for RU (see Table 4.2), it is apparent in both Figure 4.4 and 4.5 that at the shorter emission wavelengths the spectrum of SLG follows more closely the shape of the spectroscopic fluorescence emission.

In ECL experiments using opaque electrodes, the fact that light must travel a farther distance through the solution to get to the detector implies increased absorption of the emitted light by the bulk of the solution. This is exacerbated in ECL experiments, compared to fluorescence spectra, as the concentrations of ECL luminophores are typically present in the mM range rather than the μM range in fluorescence. This effect is more prominent with RU than other mediators (e.g. DPA, which emits blue light), a phenomenon that is consistent with other observations of large shifts on dyes with red emission.[29, 52] This is supported by the shift in peak emission wavelength for measurements with *filtered SLG*, with the detector above the solution at the SLG electrode at the bottom. Just as with the metal electrode measurements the light must pass through the solution before reaching the detector (see Figure 2.2B). Inner filter effects depend on both the spectral overlap between the absorbance of the species and its emission (i.e., its Stokes shift), and the concentration of the species. While the aspects of the species concentration can be alleviated by choosing appropriate conditions, usually there will be a compromise between the ECL intensity and solving inner filter effects. With increasing studies of ECL in donor-acceptor systems, [31, 32, 53, 54] it is certainly desirable to work with an electrode platform on which radical annihilation ECL can be obtained in the absence of inner filter effects. Since SLG can be wet transfer over various substrates, it offers the attractive opportunity to use this material as a flexible platform for spectroelectrochemical experiments of electrogenerated species that are not

limited to traditional ECL experiments. This also permits its use together with an inverted-microscope or for coupled SECM-ECL platforms.[55, 56]

4.5 Conclusions

We used continuous single layer graphene as a suitable electrode in non-aqueous media to study ECL luminophores from -2.4 V to +1.8 V. While SLG obtained by chemical vapor deposition showed higher electrical resistance than metal electrodes, this may be decreased with samples that are defect free or have larger grain size. SLG showed stable electrochemical behavior and was able to collect both radical cations and radical anions with high efficiency and without any apparent degradation. SLG can be polarized to produce radical cations and radical anions such that ECL emission is achieved, thus improving upon metal oxide materials as transparent electrodes. Furthermore, spectroelectrochemical studies can be improved by placing the optical detector beneath the transparent electrode, minimizing inner filter effects. SLG is an ideal transparent electrode for combining optical and electrochemical measurements, such as SECM studies to be coupled with ECL.

Table 4.1: Peak splitting for CVs displaying the differences in electrochemical behavior between SLG and metal electrodes. CVs were collected at 25 mV/s and in 0.1 M TBA.PF_6

Electrode material	DPA		RU	
	ΔE_{red} (mV)	ΔE_{ox} (mV)	ΔE_{red} (mV)	ΔE_{ox} (mV)
SLG	232	242	140	110
Gold	123	116	83	62

Table 4.2: Shift in peak emission wavelength based on electrode material, luminophore and whether spectral data was collected through the solution or not

Electrode Material	DPA	RU
	$\Delta\lambda$ (nm)	$\Delta\lambda$ (nm)
SLG	0.9 ± 1.0	1.0 ± 0.09
SLG - Filtered	--	8.8 ± 0.09
Gold/Platinum	2.0 ± 1.0	10.9 ± 0.3

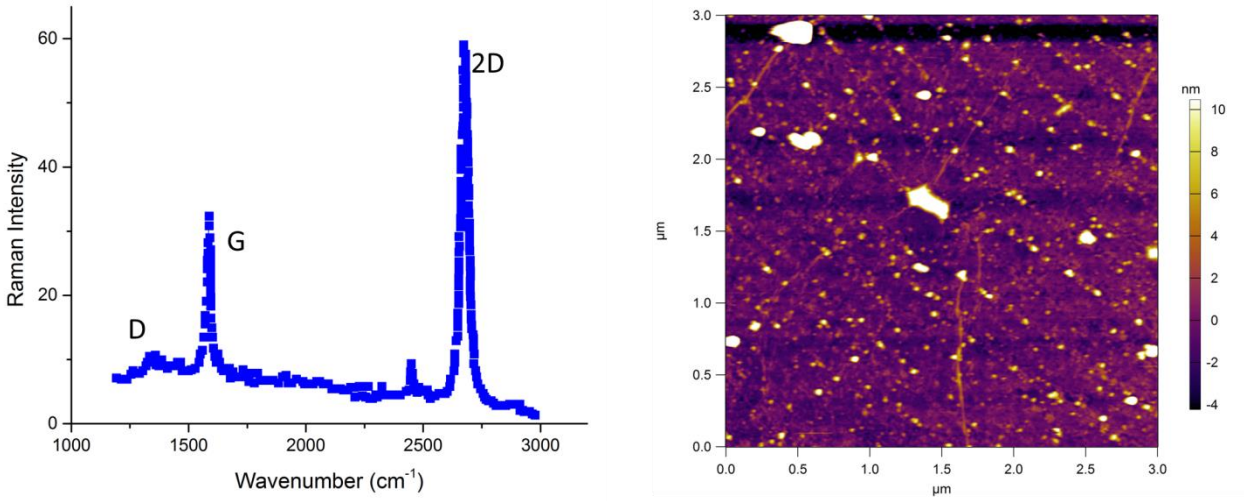

Figure 4.1: Raman spectrum (left) of a typical SLG sample where the 2D band is ~twice as intense as the G band, which indicates that it is predominately monolayer coverage. The presence of the D peak indicates that the sample is not defect free. A tapping mode AFM image (right) shows a sample of SLG on glass including roughness from the glass, pieces of dust and wrinkles from the wet transfer process.

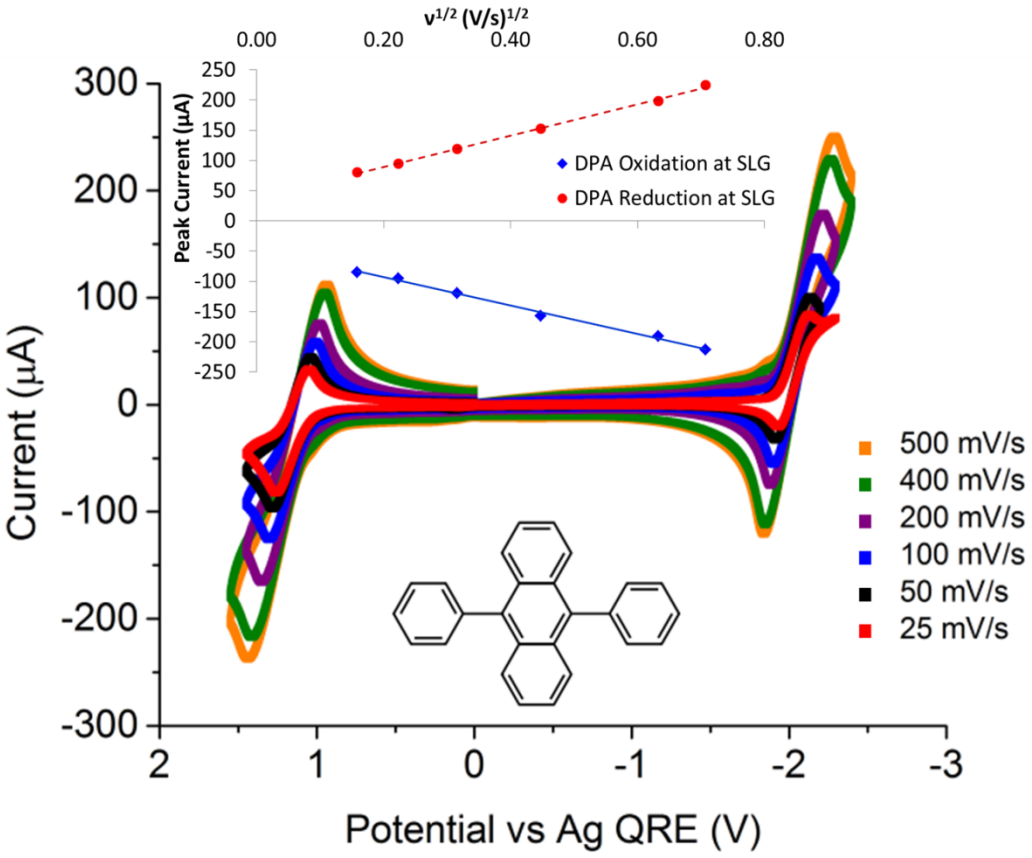

Figure 4.2: CVs of 1 mM DPA in 100 mM TBA.PF_6 in acetonitrile using a 0.28 cm^0 SLG electrode showing scan rate dependence in agreement with the Randles-Sevcik equation with a diffusion coefficient of 8.3 x 10^{-6} cm^2/s.[26] The bottom inset shows the structure of DPA.

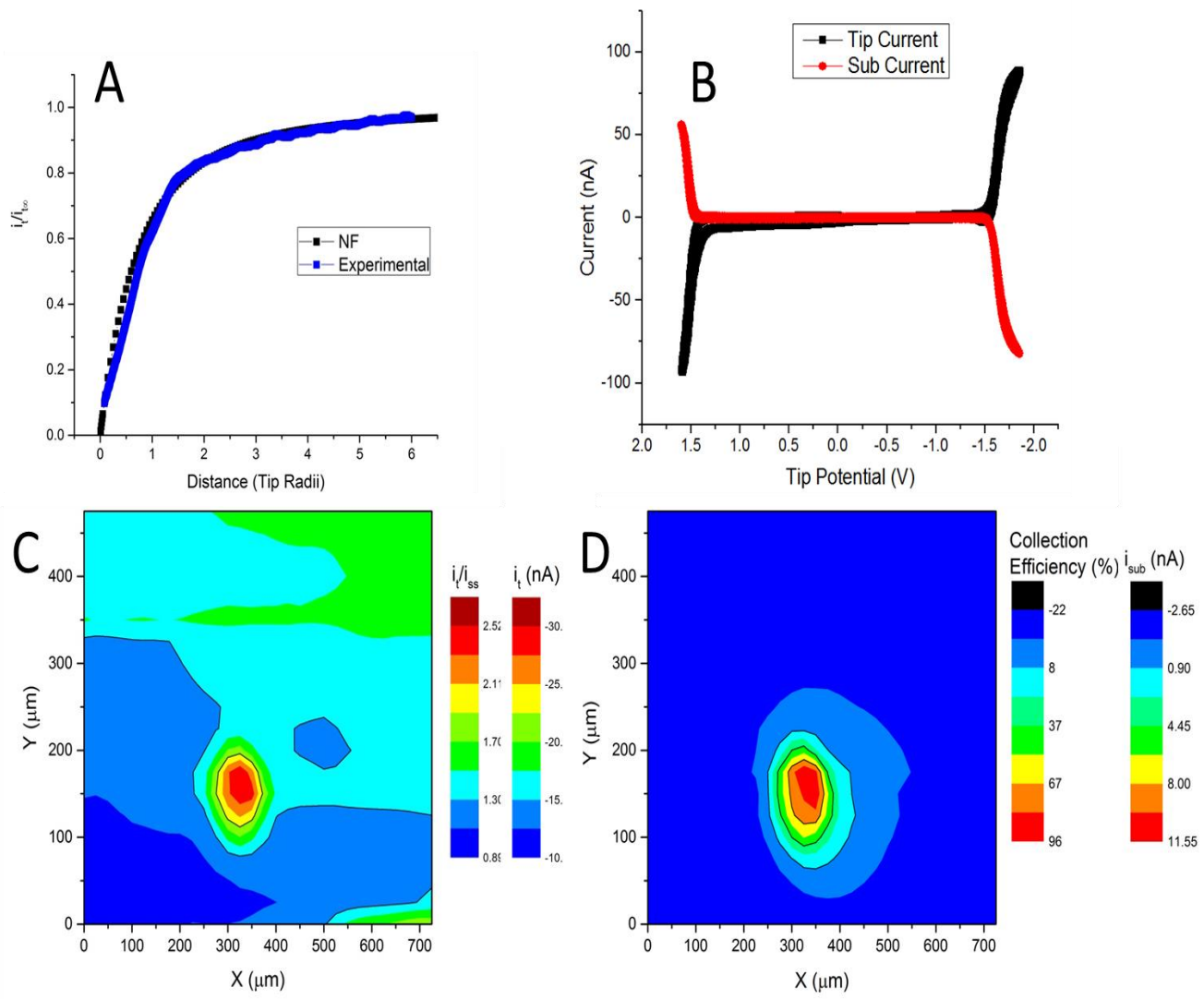

Figure 4.3: SECM image using DPA as a mediator to probe a partially insulated SLG electrode. The 50 μm gold tip was approached at a rate of 60 μm·s^{-1} to 10 μm above a region of PTFE for negative feedback (A) and then aligned above a region of exposed SLG. An image was obtained for the feedback current at the tip (C) and the collection current at the SLG (D) expressed as both absolute and normalized currents.

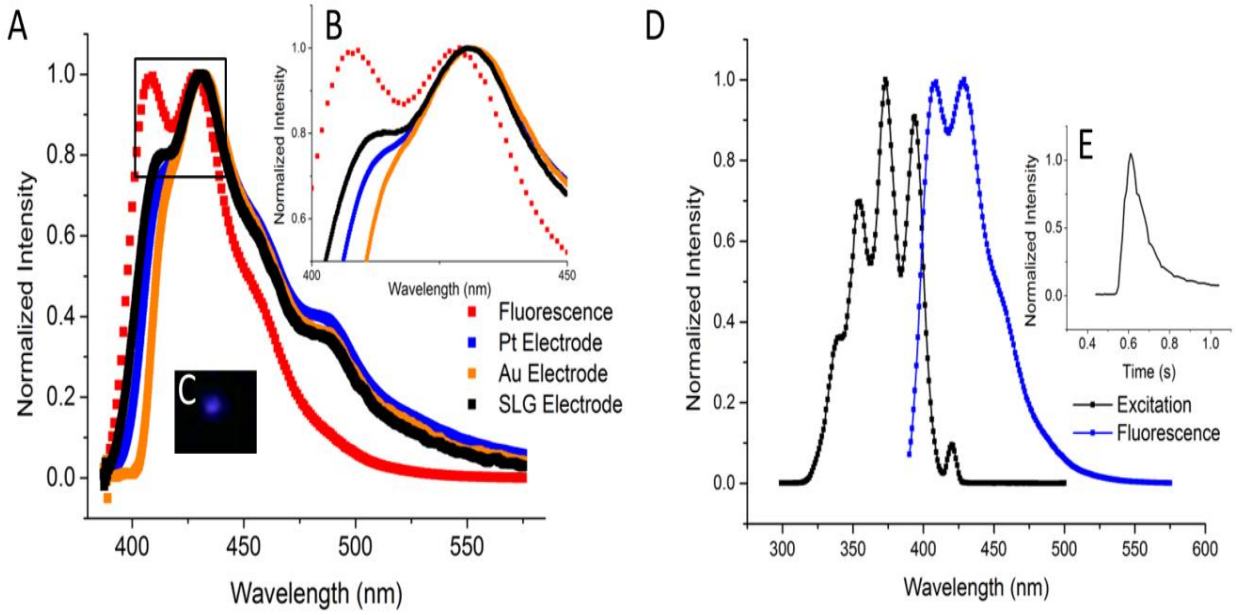

Figure 4.4: Fluorescence and ECL spectra of DPA (A), focused on the region of interest (B) highlighting the minimal inner filter effects when using a blue emitter. An image of the emission is shown in (C) with the contrast altered for clarity due to poor sensitivity of the camera. The excitation and emission spectra (D) show ~ 30 nm window of overlap. ECL spectra were collected with 40 second integration a produced via chronoamperametry with 0.5 second pulses, a transient of which is shown in (E).

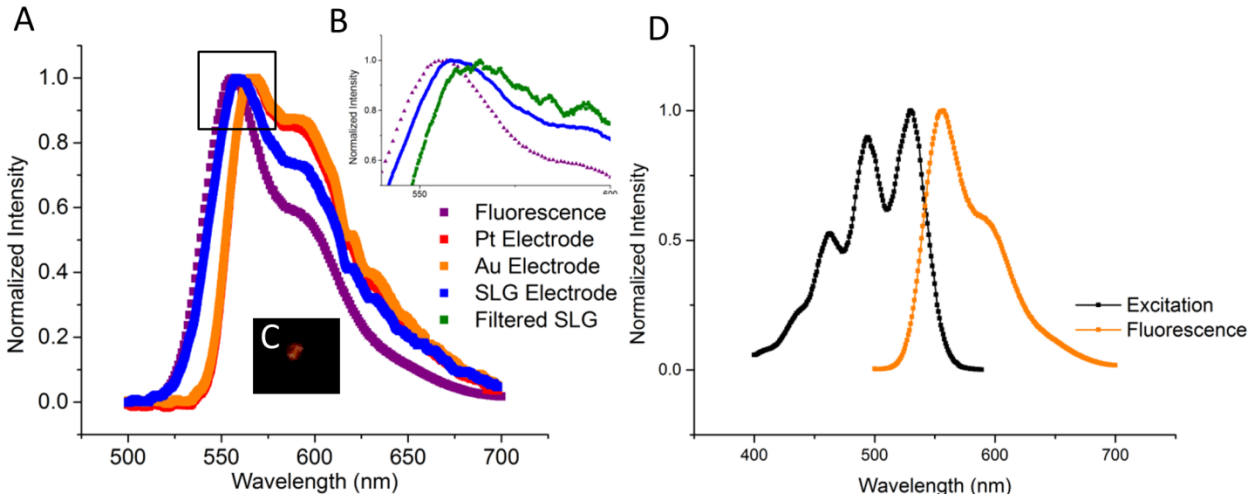

Figure 4.5: Fluorescence and ECL spectra of RU using various electrodes collected with the shutter open for 40 seconds and electrochemical pulses every 0.5 seconds (A). Zooming in on the peak emission region (B) shows the difference in emission wavelength between fluorescence and a SLG electrode with the measurements taken both above (blue) and below (green) the solution. An image of the emission is shown in (C) with the contrast slightly enhanced. The excitation and emission spectra of RU (D) show a large (~60 nm) window of overlap, the cause of inner filter effects.

Chapter 5: Conclusions

The results of this work were mixed. Work with SLG was initially limited by the quality and stability of samples. SLG electrodes often had a density of defects, represented by a large D band in the Raman spectrum, and become extremely resistive in potential windows between +1.5 V and -1 V versus a quasi-reference electrode. This makes radical annihilation ECL completely impossible as the window is too small to produce radical anions and radical cations of high enough energy to emit visible light. Thus, great care must be taken in the preparation of SLG samples. Copper foil must be thoroughly washed and minimally wrinkled before being inserted in the CVD. After growth the sample should be coated with PMMA as soon as possible to reduce the chance of degradation from reaction with species in the air and to add a layer of protection from scratches and other mechanical defects. To improve the stability of SLG electrodes during experiments the PTFE layer is very important. This protects samples during the experiment in a similar way that PMMA does prior to transfer steps. PTFE also sits between the SLG and o-ring of the SECM cell and helps keep the SLG continuous which maintains the electrical connection.

Once SLG samples are of a high enough quality for ECL experiments they are an ideal electrode material. There is more resistance than with metal electrodes, but this is mostly avoided with slow scan rates. Since all experiments must be done in a glovebox there is a major evaporation issue. This makes it almost impossible to be confident about the concentration of the solution. The bigger issue, though, is that as the solution level decreases it can go beneath where the reference and counter electrode are. If there is no reference electrode in the solution and an experiments are attempted with a SLG electrode it will be destroyed. This issue plagued most experiments as the lights were off for detecting ECL and all equipment had to be shut off in

order to add more solvent. There may not be a convenient way of addressing this issue but it can be a significant hold up in experiments.

In this work CTRIPs was never experimentally observed. Theoretically the pulsing experiments should have produced CTRIPs as the annihilation energy is equivalent as that previously observed.[41] This line of experimentation should not be pursued but replicating the experiments without as many different potentials is a good way to become proficient in producing and measuring radical annihilation ECL. It does not seem worthwhile to pursue CTRIPs using an SLG graphene with SECM until the emission can be confirmed in some other way. Using two large electrodes to achieve steady state radical annihilation ECL and try to observe CTRIPs would be a better start to this work. This will make emission visible by eye and will make detection easier. Specifically, the Avantes spectrometer will be able to be used to obtain a spectrum of the emission to concretely show that the pre-emission observed by Rodriguez-Lopez et al. is of a higher wavelength

The most interesting aspect of this work that should be explored is combinatorial SECM-ECL images. This work shows that SLG electrodes can collect radical anions when held at 0 V and both a tip feedback image and substrate collection current image can be obtained. Since the SLG electrode was not biased to E_{ox} no ECL was produced during these measurements. One image was attempted with the substrate biased to E_{ox} with tip scanning at E_{red}, scanning the same area as in Figure 4.3. This did not yield an image of the SLG spot surrounded by PTFE, however this should be possible. Further, if this is done with the PMT on a third image can be collected by plotting the ECL intensity. It will be difficult to ensure that all three images correlate to the same scale, but it should be possible. In terms of experimental preparation, the SECM tips used will need to be approached quite closely and therefore should have an RG < 4, though the important

issue will be for it to be completely flat. These tips may be best, and most reproducibly, produced with HF etching. One of the advantages would be to have the substrate at a slight underpotential and areas of higher electrochemical activity (e.g. grain boundaries, nanoparticles) will produce more light. While not all of the work was successful, this work has shown that SLG is an ideal transparent electrode for non-aqueous electrochemical studies coupled with optical measurements.

REFERENCES

1. Novoselov, K. S.; Geim, A. K.; Morozov, S. V.; Jiang, D.; Zhang, Y.; Dubonos, S. V.; Grigorieva, I. V.; Firsov, A. A., Electric Field Effect in Atomically Thin Carbon Films. *Science* 2004, 306, 666-669.

2. Novoselov, K. S.; Jiang, D.; Schedin, F.; Booth, T. J.; Khotkevich, V. V.; Morozov, S. V.; Geim, A. K., Two-Dimensional Atomic Crystals. *Proceedings of the National Academy of Sciences of the United States of America* 2005, 102, 10451-10453.

3. Castro Neto, A. H.; Guinea, F.; Peres, N. M. R.; Novoselov, K. S.; Geim, A. K., The Electronic Properties of Graphene. *Reviews of Modern Physics* 2009, 81, 109-162.

4. Geim, A. K.; Novoselov, K. S., The rise of graphene. *Nature Materials* 2007, 6, 183-191.

5. Ritzert, N. L.; Rodriguez-Lopez, J.; Tan, C.; Abruna, H. D., Kinetics of Interfacial Electron Transfer at Single-Layer Graphene Electrodes in Aqueous and Nonaqueous Solutions. *Langmuir* 2013, 29, 1683-1694.

6. Tan, C.; Rodriguez-Lopez, J.; Parks, J. J.; Ritzert, N. L.; Ralph, D. C.; Abruna, H. D., Reactivity of Monolayer Chemical Vapor Deposited Graphene Imperfections Studied Using Scanning Electrochemical Microscopy. *Acs Nano* 2012, 6, 3070-3079.

7. Dreyer, D. R.; Park, S.; Bielawski, C. W.; Ruoff, R. S., The Chemistry of Graphene Oxide. *Chemical Society Reviews* 2010, 39, 228-240.

8. Hummers, W. S.; Offeman, R. E., Preparation of Graphitic Oxide. *Journal of the American Chemical Society* 1958, 80, 1339-1339.

9. Kim, D. Y.; Sinha-Ray, S.; Park, J. J.; Lee, J. G.; Cha, Y. H.; Bae, S. H.; Ahn, J. H.; Jung, Y. C.; Kim, S. M.; Yarin, A. L.; Yoon, S. S., Self-Healing Reduced Graphene Oxide Films by Supersonic Kinetic Spraying. *Advanced Functional Materials* 2014, 24, 4986-4995.

10. Ferrari, A. C.; Meyer, J. C.; Scardaci, V.; Casiraghi, C.; Lazzeri, M.; Mauri, F.; Piscanec, S.; Jiang, D.; Novoselov, K. S.; Roth, S.; Geim, A. K., Raman spectrum of graphene and graphene layers. *Physical Review Letters* 2006, 97, 4.

11. Li, X. S.; Cai, W. W.; An, J. H.; Kim, S.; Nah, J.; Yang, D. X.; Piner, R.; Velamakanni, A.; Jung, I.; Tutuc, E.; Banerjee, S. K.; Colombo, L.; Ruoff, R. S., Large-Area Synthesis of High-Quality and Uniform Graphene Films on Copper Foils. *Science* 2009, 324, 1312-1314.

12. Lim, C. X.; Hoh, H. Y.; Ang, P. K.; Loh, K. P., Direct Voltammetric Detection of DNA and pH Sensing on Epitaxial Graphene: An Insight into the Role of Oxygenated Defects. *Analytical Chemistry* 2010, 82, 7387-7393.

13. Zhan, D.; Yan, J. X.; Lai, L. F.; Ni, Z. H.; Liu, L.; Shen, Z. X., Engineering the Electronic Structure of Graphene. *Advanced Materials* 2012, 24, 4055-4069.

14. Bard, A. J.; Denuault, G.; Lee, C.; Mandler, D.; Wipf, D. O., Scanning Electrochemical Microscopy - A new Technique for the Characterization and Modification of Surfaces. *Accounts of Chemical Research* 1990, 23, 357-363.

15. Rodriguez-Lopez, J.; Ritzert, N. L.; Mann, J. A.; Tan, C.; Dichtel, W. R.; Abruna, H. D., Quantification of the Surface Diffusion of Tripodal Binding Motifs on Graphene Using Scanning Electrochemical Microscopy. *Journal of the American Chemical Society* 2012, 134, 6224-6236.

16. Mirkin, M. V.; Nogala, W.; Velmurugan, J.; Wang, Y. X., Scanning Electrochemical Microscopy in the 21st Century. Update 1: Five Years After. *Physical Chemistry Chemical Physics* 2011, 13, 21196-21212.

17. Chen, P. H.; Fryling, M. A.; McCreery, R. L., Electron-Transfer Kinetics at Modified Carbon Electrode Surfaces - The Role of Specific Surface Sites. *Analytical Chemistry* 1995, 67, 3115-3122.

18. Kanoufi, F.; Bard, A. J., Electrogenerated Chemiluminescence. 65. An Investigation of the Oxidation of Oxalate by Tris(polypyridine) Ruthenium Complexes and the Effect of the Electrochemical Steps on the Emission Iintensity. *Journal of Physical Chemistry B* 1999, 103, 10469-10480.

19. Miao, W. J., Electrogenerated Chemiluminescence and its Biorelated Applications. *Chemical Reviews* 2008, 108, 2506-2553.

20. Pittman, T. L.; Miao, W. J., Examination of Electron Transfer Through DNA Using Electrogenerated Chemiluminescence. *Journal of Physical Chemistry C* 2008, 112, 16999-17004.

21. Zhou, J. G.; Booker, C.; Li, R. Y.; Zhou, X. T.; Sham, T. K.; Sun, X. L.; Ding, Z. F., An Electrochemical Avenue to Blue Luminescent Nanocrystals from Multiwalled Carbon Nanotubes (MWCNTs). *Journal of the American Chemical Society* 2007, 129, 744-745.

22. Boto, K. G.; Bard, A. J., Electrogenerated Chemiluminescence .24. Electrochemistry and Electrogenerated Chemiluminescence of 9,10-Dichloro-9,10-Dihydro-9,10-Diphenylanthracene. *Journal of Electroanalytical Chemistry* 1975, 65, 945-962.

23. Brilmyer, G. H.; Bard, A. J., Electrogenerated Chemi-luminescence 36. Production of Steady Direct-Current ECL in Thin-Layer and Flow Cells. *Journal of the Electrochemical Society* 1980, 127, 104-110.

24. Laser, D.; Bard, A. J., Electrogenerated Chemiluminescence .23. Operation and Lifetime of ECL Devices. *Journal of the Electrochemical Society* 1975, 122, 632-640.

25. McCord, P.; Bard, A. J., Electrogenerated Chemiluminescence .54. Electrogenerated Chemiluminescence of Ruthenium(II) 4,4'-Diphenyl-2,2'-Bipyridine and Ruthenium(II) 4,7-

Diphenyl-1,10-Phenanthroline Systems in Aqueous and Acetonitrile Solutions. *Journal of Electroanalytical Chemistry* 1991, 318, 91-99.

26. Miller, C. J.; McCord, P.; Bard, A. J., Study of Langmuir Monolayers of Ruthenium Complexes and Their Aggregation by Electrogenerated Chemiluminescence. *Langmuir* 1991, 7, 2781-2787.

27. Nepomnyashchii, A. B.; Bard, A. J., Electrochemistry and Electrogenerated Chemiluminescence of BODIPY Dyes. *Accounts of Chemical Research* 2012, 45, 1844-1853.

28. Santhana.Ks; Bard, A. J., Chemiluminescence of Electrogenerated 9,10-Diphenylanthracene Anion Radical. *Journal of the American Chemical Society* 1965, 87, 139-&.

29. Shen, M.; Rodriguez-Lopez, J.; Huang, J.; Liu, Q. A.; Zhu, X. H.; Bard, A. J., Electrochemistry and Electrogenerated Chemiluminescence of Dithienylbenzothiadiazole Derivative. Differential Reactivity of Donor and Acceptor Groups and Simulations of Radical Cation-Anion and Dication-Radical Anion Annihilations. *Journal of the American Chemical Society* 2010, 132, 13453-13461.

30. Tokeltak.Ne; Hemingwa.Re; Bard, A. J., Electrogenerated Chemiluminescence .13. Electrochemical and Electrogenerated Chemiluminescence Studies of Ruthenium Chelates. *Journal of the American Chemical Society* 1973, 95, 6582-6589.

31. Richter, M. M., Electrochemiluminescence (ECL). *Chemical Reviews* 2004, 104, 3003-3036.

32. Forster, R. J.; Bertoncello, P.; Keyes, T. E., Electrogenerated Chemiluminescence. In *Annual Review of Analytical Chemistry*, Annual Reviews: Palo Alto, 2009; Vol. 2, pp 359-385.

33. Ritzert, N. L.; Li, W.; Tan, C.; Rodriguez-Calero, G. G.; Rodriguez-Lopez, J.; Hernandez-Burgos, K.; Conte, S.; Parks, J. J.; Ralph, D. C.; Abruna, H. D., Single Layer Graphene as an Electrochemical Platform. *Faraday Discussions* 2014.

34. McCreery, R. L., Advanced Carbon Electrode Materials for Molecular Electrochemistry. *Chemical Reviews* 2008, 108, 2646-2687.

35. Edwards, M. A.; Bertoncello, P.; Unwin, P. R., Slow Diffusion Reveals the Intrinsic Electrochemical Activity of Basal Plane Highly Oriented Pyrolytic Graphite Electrodes. *Journal of Physical Chemistry C* 2009, 113, 9218-9223.

36. Dumitrescu, I.; Dudin, P. V.; Edgeworth, J. P.; Macpherson, J. V.; Unwin, P. R., Electron Transfer Kinetics at Single-Walled Carbon Nanotube Electrodes using Scanning Electrochemical Microscopy. *Journal of Physical Chemistry C* 2010, 114, 2633-2639.

37. Sartin, M. M.; Camerel, F.; Ziessel, R.; Bard, A. J., Electrogenerated Chemiluminescence of B(8)amide: A BODIPY-Based Molecule with Asymmetric ECL Transients. *Journal of Physical Chemistry C* 2008, 112, 10833-10841.

38. Wu, Z. C.; Chen, Z. H.; Du, X.; Logan, J. M.; Sippel, J.; Nikolou, M.; Kamaras, K.; Reynolds, J. R.; Tanner, D. B.; Hebard, A. F.; Rinzler, A. G., Transparent, Conductive Carbon Nanotube Films. *Science* 2004, 305, 1273-1276.

39. Ellmer, K., Past Achievements and Future Challenges in the Development of Optically Transparent Electrodes. *Nature Photonics* 2012, 6, 808-816.

40. Hecht, D. S.; Hu, L. B.; Irvin, G., Emerging Transparent Electrodes Based on Thin Films of Carbon Nanotubes, Graphene, and Metallic Nanostructures. *Advanced Materials* 2011, 23, 1482-1513.

41. Rodriguez-Lopez, J.; Shen, M.; Nepomnyashchii, A. B.; Bard, A. J., Scanning Electrochemical Microscopy Study of Ion Annihilation Electrogenerated Chemiluminescence of Rubrene and Ru(bpy)(3) (2+). *Journal of the American Chemical Society* 2012, 134, 9240-9250.

42. Collinson, M. M.; Wightman, R. M., Observation of Individual Chemical Reactions in Solution. *Science* 1995, 268, 1883-1885.

43. Kanoufi, F.; Cannes, C.; Zu, Y. B.; Bard, A. J., Scanning electrochemical microscopy. 43. Investigation of oxalate oxidation and electrogenerated chemiluminescence across the liquid-liquid interface. *Journal of Physical Chemistry B* 2001, 105, 8951-8962.

44. Fan, F. R. F.; Cliffel, D.; Bard, A. J., Scanning electrochemical microscopy. 37. Light emission by electrogenerated chemiluminescence at SECM tips and their application to scanning optical microscopy. *Analytical Chemistry* 1998, 70, 2941-2948.

45. Gosavi, S.; Marcus, R. A., A model for charge transfer inverse photoemission. *Electrochimica Acta* 2003, 49, 3-21.

46. Rodriguez-Lopez, J.; Alpuche-Aviles, M. A.; Bard, A. J., Selective Insulation with Poly(tetrafluoroethylene) of Substrate Electrodes for Electrochemical Background. Reduction in Scanning Electrochemical Microscopy. *Analytical Chemistry* 2008, 80, 1813-1818.

47. Kakaei, K., One-pot electrochemical synthesis of graphene by the exfoliation of graphite powder in sodium dodecyl sulfate and its decoration with platinum nanoparticles for methanol oxidation. *Carbon* 2013, 51, 195-201.

48. Brulle, T.; Ju, W. B.; Niedermayr, P.; Denisenko, A.; Paschos, O.; Schneider, O.; Stimming, U., Size-Dependent Electrocatalytic Activity of Gold Nanoparticles on HOPG and Highly Boron-Doped Diamond Surfaces. *Molecules* 2011, 16, 10059-10077.

49. Maness, K. M.; Bartelt, J. E.; Wightman, R. M., Effects of Solvent and Ionic-Strength on the Electrochemiluminescence Of 9,10-Diphenylanthracene

Journal of Physical Chemistry 1994, 98, 3993-3998.

50. Wightman, R. M.; Curtis, C. L.; Flowers, P. A.; Maus, R. G.; McDonald, E. M., Imaging Microelectrodes with High-Frequency Electrogenerated Chemiluminescence. *Journal of Physical Chemistry B* 1998, 102, 9991-9996.

51. Lefrou, C.; Cornut, R., Analytical Expressions for Quantitative Scanning Electrochemical Microscopy (SECM). *Chemphyschem* 2010, 11, 547-556.

52. Shen, M.; Rodriguez-Lopez, J.; Lee, Y. T.; Chen, C. T.; Fan, F. R. F.; Bard, A. J., Electrochemistry and Electrogenerated Chemiluminescence of a Novel Donor-Acceptor FPhSPFN Red Fluorophore. *Journal of Physical Chemistry C* 2010, 114, 9772-9780.

53. Brilmyer, G. H.; Bard, A. J., Electrogenerated Chemiluminescence 36. Production of Steady Direct-Current ECL in Thin-Layer and Flow Cells. *Journal of the Electrochemical Society* 1980, 127, 104-110.

54. Collinson, M. M.; Wightman, R. M.; Pastore, P., Evaluation of Ion-Annihilation Reaction-Kinetics Using High-Frequency Generation of Electrochemiluminescence. *Journal of Physical Chemistry* 1994, 98, 11942-11947.

55. Hill, C. M.; Clayton, D. A.; Pan, S., Combined Optical and Electrochemical Methods for Studying Electrochemistry at the Single Molecule and Single Particle Level: Recent Progress and Perspectives. *Physical Chemistry Chemical Physics* 2013, 15, 20797-20807.

56. Lei, R.; Stratmann, L.; Schafer, D.; Erichsen, T.; Neugebauer, S.; Li, N.; Schuhmann, W., Imaging Biocatalytic Activity of Enzyme-Polymer Spots by Means of Combined Scanning

Electrochemical Microscopy/Electrogenerated Chemiluminescence. *Analytical Chemistry* 2009, 81, 5070-5074.